Higher-order corrections to electron-nucleus bremsstrahlung cross sections above a few MeV

A. Mangiarotti* and M. N. Martins
Instituto de Física da Universidade de São Paulo, Rua do Matão 187, 05508-090 São Paulo, Brazil
(Received 5 July 2016; published 15 August 2016)

Despite the fact that the first calculations of nuclear bremsstrahlung cross sections were performed for relativistic electrons more than 80 years ago by Sauter, Bethe and Heitler, and Racah, a fully satisfactory solution to this problem is still missing up to the present day. Numerical approaches are impractical for electrons with energies above a few MeV because they require a prohibitively large number of partial waves. Analytic formulae need to describe simultaneously and accurately the interaction with the Coulomb field of the nucleus and the screening effect of the atomic electrons. In the present paper, a state-of-the-art analytic calculation will be discussed. In particular, higher-order corrections to the interaction with the Coulomb field of the nucleus, a subject seldom tackled in the past, are included and compared extensively with published data. The emerged difficulties will be highlighted, but unfortunately they can be overcome only with future large coordinated theoretical and experimental efforts.

DOI: 10.1103/PhysRevA.94.022708

I. INTRODUCTION

The theory of bremsstrahlung emission has been developed since about 100 years ago starting with the first semiclassical attempts by Sommerfeld shortly after the introduction of the Bohr atomic model. The first nonrelativistic quantum calculation was published by Sommerfeld in 1931 [1]. A relativistic treatment was first given in 1934, independently, by Sauter [2], Bethe and Heitler [3,4], and Racah [5]. Since then, a large number of calculations has been reported. But even nowadays, as we will show in the present paper, a fully satisfactory solution for nuclear bremsstrahlung by few-MeV electrons is not available. The various theories can be divided in two large classes: analytic formulae and numerical approaches. The present paper focuses just on the former.

We have found 28 analytic formulae for nuclear bremsstrahlung only, valid under different approximations. This is not the place for a complete discussion (a review will be published shortly elsewhere [6]). Here it is important to stress the main difficulty at the base of such a large proliferation of theoretical works. Because radiative corrections to bremsstrahlung (i.e., genuine quantum electrodynamics effects) are small [7], Fermi's "golden rule" is fully adequate to calculate accurately the triple differential cross section. However, the initial and final electron wave functions are difficult to obtain because it is necessary to consider that the Coulomb field of the nucleus is screened by the atomic electrons. Even for a pure Coulomb field (which is an inadequate approximation for the bremsstrahlung emission especially of low-energy photons) the eigenfunctions of the Dirac equation for the continuous part of the energy spectrum cannot be obtained in closed form. For high-Z atoms, where the bremsstrahlung emission is stronger, the effect of screening can only be described appropriately with an atomic form factor obtained from a Dirac-Hartree-Fock numerical approach. Here we will show the results for a state-of-the art analytic calculation for bremsstrahlung in the Coulomb field of the nucleus modified by the presence of the electronic cloud of the atom. We will include second-order corrections to the interaction with the Coulomb field of the nucleus, following a recent work by Haug [8], and analyze thoroughly the consequences for double and single differential cross sections, especially in comparison with the available experimental data, which are scarce and old. Unfortunately, however, only partial conclusions are possible without future large coordinated theoretical and experimental efforts.

The main objection to the present work, especially when confronted with the difficulties that will become apparent in the comparison to experimental data for high-Z elements, is the existence of numerical methods that are virtually exact, because they employ initial and final electron wave functions obtained from the solution of the Dirac equation in a realistic central potential including the screening effect of the atomic electrons. These approaches are based on partial wave expansions and are indeed considered the best calculations available. They have been refined over the years by Tseng and Pratt [9]. However, because the number of components needed to obtain an accurate cross section for few-MeV electrons is rather high, the reference tabulations by Tseng and Pratt [10] stopped at electron kinetic energies of $T_{e1} = 2$ MeV. Pratt *et al.* have later introduced a sampling procedure that avoids the direct calculation of all the partial wave components [11], but only exploratory calculations have been published for Al and U at $T_{e1} = 5$ and 10 MeV. Recently, Yerokhin and Surzhykov [12] have developed a completely independent computer code and introduced an important improvement in the evaluation of the strongly oscillating integrals appearing in the coefficients of the partial wave expansion. Their results confirm the ones by Tseng and Pratt [10], being typically lower by at most 1% because they use an improved central potential; still Yerokhin and Surzhykov [12] stopped at 3 MeV. It is important to remember that the bremsstrahlung matrix element depends on both the initial and final electron wave functions and hence the number of contributions that have to be included scales with the square of the number of partial wave components. For this reason, the number of terms in the matrix element increases exponentially with energy [13]. Jakubassa-Amundsen [14,15] has proposed a mixed approach valid only for the cross section at the high-energy end of the bremsstrahlung photon spectrum (called the "tip" in the

*alessio@if.usp.br

literature) by coupling an analytic wave function for the initial state to a partial wave expansion for the final one (where the electron has a very low kinetic energy and feels strongly the effect of the screened Coulomb field). Since here we are interested in the full radiated spectrum and we want to reach higher electron energies, in particular to study the high-energy limit of the Coulomb correction, we cannot rely on these exact numerical methods.

As a last warning, we remind the reader that electron-electron bremsstrahlung exists as well, but it is important for very low-Z elements, which fall outside the scope of the present work.

The paper is structured as follows. The analytic formulae are developed in Sec. II, their numerical implementation is described in Sec. III, and some general features are discussed in Sec. IV. A comparison with the experimental data is performed for double differential cross sections at a few MeV and for single differential cross sections at hundreds of MeV in Secs. V and VI, respectively. Finally, the conclusions are drawn in Sec. VII.

Throughout the text, the abbreviations adopted are the triple differential cross section (TDCS), double differential cross section (DDCS), single differential cross section (SDCS), partial differential equation (PDE), atomic form factor (AFF), leading order (LO), and next-to-leading order (NLO).

II. HIGHER-ORDER CORRECTIONS TO ANALYTIC FORMULAE

As mentioned above, the main limitation of all analytic formulae is the difficulty to find an accurate expression of the eigenfunctions of the Dirac equation for scattering from the Coulomb field of the nucleus. Moreover, the screening effect of the atomic electrons also needs to be handled. For a pure Coulomb field, the best analytic wave functions have been found independently by Furry [16] and Sommerfeld and Maue [17] (they will be called the Furry-Sommerfeld-Maue wave functions here, but in most of the literature they are identified simply as the Sommerfeld-Maue wave functions). On the other hand, the effect of screening cannot be included easily in the Furry-Sommerfeld-Maue wave functions, but can be easily accounted for in the Born approximation (which does not describe accurately the interaction with the Coulomb field of the nucleus).

A. The general Olsen-Maximon-Wergeland additivity rule

As mentioned, Fermi's "golden rule" is fully adequate for treating nuclear bremsstrahlung. The matrix element to be evaluated contains an integral of the initial- and final-state wave functions over the whole space. However, as noted by Bethe and Maximon [18], close to the nucleus an accurate description of the interaction with a pure Coulomb field is most important, while far from the nucleus the effect of screening is most relevant so that the Coulomb field is strongly reduced and hence amenable to a Born-approximation approach: thus, over all space, it is never necessary to deal with both difficulties simultaneously. This observation was exploited in detail by Olsen, Maximon, and Wergeland [19], who could prove, within the Wentzel-Kramers-Brillouin (WKB) approximation, that, at high energies (compared with the rest mass of the electron) and for cross sections that are integrated over the final electron solid angle, the screening correction is additive:

$$\left(\frac{d^2\sigma}{dk\,d\Omega_k}\right)^{\text{screened}}_{\text{exact}} = \left(\frac{d^2\sigma}{dk\,d\Omega_k}\right)^{\text{no screening}}_{\text{exact}} + \left[\left(\frac{d^2\sigma}{dk\,d\Omega_k}\right)^{\text{screened}}_{\text{Born}} - \left(\frac{d^2\sigma}{dk\,d\Omega_k}\right)^{\text{no screening}}_{\text{Born}}\right]. \tag{1}$$

The first term on the right-hand side of Eq. (1) is the exact cross section in a pure Coulomb field, while the second contains the correction due to screening evaluated from the Born approximation. A more detailed discussion of Eq. (1) can be found in Refs. [20–22]. Here we will call this property the Olsen-Maximon-Wergeland additivity rule.

In the present work, we will use Eq. (1) and improve as far as possible each term. As suggested by Haug [8], the exact cross section in a pure Coulomb field is approximated with the Elwert-Haug expression [23], obtained with the Furry-Sommerfeld-Maue wave functions [16,17], corrected to the next-to-leading order with the formula by Roche, Ducos, and Proriol [24]. We refine the work by Haug [8] by using the TDCS from the Born approximation obtained by Maximon, de Miniac, Aniel, and Ganz [25] with the best non-relativistic Hartree-Fock AFFs available, compiled by Hubbell and collaborators [26]. We discuss briefly each term with the intent of clarifying the limitations involved.

B. The Born approximation

In the Born approximation, the electron wave function is expanded as

$$\Psi = \phi_0 + (\alpha\,Z)\,\phi_1 + (\alpha\,Z)^2\,\phi_2 + \cdots \tag{2}$$

where the expansion parameter is $\alpha\,Z$ (with α the fine-structure constant) and the expansion point ϕ_0 is a plane wave, i.e., representing a particle that is free. The other terms in Eq. (2) can be obtained iteratively by solving the Dirac equation by means of the Green's-function method. However, only the term of order $\alpha\,Z$ is practically usable for calculating the bremsstrahlung TDCS because of divergences. When Eq. (2) is stopped after the term of order $\alpha\,Z$, it is called the first Born approximation. The plane wave does not contribute to the TDCS because a free electron cannot radiate a photon due to energy-momentum conservation. It is rather obvious that the first Born approximation can be reasonably accurate only if the interaction of the electron with the nucleus is weak. In general, a particle is never free from a Coulomb field; but, because of the screening, the notion of a weak interaction can be applied far from the nucleus.

The first Born approximation was the method originally employed, independently, by Sauter [2], Bethe and Heitler [3,4], and Racah [5]. Only the work by Bethe and Heitler [3,4] dealt with screening and because their result was more general became the most widely cited: it is commonly referred as the Bethe-Heitler formula. However, we do not use their expression for the TDCS because it is affected by the

cancellation between different terms to such a high degree that its evaluation is numerically challenging above tens of MeV [25]. Maximon, de Miniac, Aniel, and Ganz [25] were able to find a mathematically equivalent expression that is not affected by this cancellation between different terms:

$$\frac{d^3\sigma}{dk\,d\Omega_k\,d\Omega_{p_2}} = \frac{\alpha\,Z^2\,r_0^2}{(2\pi)^2}\,\frac{p_2}{k\,p_1}\,\frac{[1-F(q)]^2}{q^4}[8\,k^2\,\epsilon_1\,\epsilon_2\,\xi\,\eta\,(\boldsymbol{u}-\boldsymbol{v})^2 + 16\,\epsilon_1^2\,\epsilon_2^2\,(\xi\,\boldsymbol{u}-\eta\,\boldsymbol{v})^2 - 4\,q^2\,(\epsilon_1\,\xi\,\boldsymbol{u}-\epsilon_2\,\eta\,\boldsymbol{v})^2] \quad (3)$$

where

$$\xi = \frac{1}{2\,\epsilon_1\,d_1}, \quad \eta = \frac{1}{2\,\epsilon_2\,d_2}, \quad (4a)$$

$$d_1 = \epsilon_1 - p_1\cos\theta_1, \quad d_2 = \epsilon_2 - p_2\cos\theta_2, \quad (4b)$$

$$\boldsymbol{q} = \boldsymbol{p}_1 - \boldsymbol{p}_2 - \boldsymbol{k}, \quad (4c)$$

and the symbols have the following meaning: ϵ_1 (ϵ_2) is the initial (final) electron energy, $\boldsymbol{p}_1$ ($\boldsymbol{p}_2$) is the initial (final) electron momentum vector, and $\boldsymbol{k}$ is the radiated photon momentum vector, all expressed in units of $m_e\,c^2$ or of $m_e\,c$, according to the correct physical dimensions, and θ_1, θ_2, $\boldsymbol{u}$, $\boldsymbol{v}$, $F(q)$, and r_0 are the angle between $\boldsymbol{p}_1$ and $\boldsymbol{k}$, the angle between $\boldsymbol{p}_2$ and $\boldsymbol{k}$, the component of $\boldsymbol{p}_1$ perpendicular to $\boldsymbol{k}$, the component of $\boldsymbol{p}_2$ perpendicular to $\boldsymbol{k}$, the AFF, and the classical electron radius, respectively. The vector $\boldsymbol{q}$ is the momentum transferred to the nucleus that recoils after the emission of the photon (in units of $m_e\,c$). Its modulus is indicated by q and called the momentum transfer.

As shown already by Bethe and Heitler [3], two necessary conditions for the first Born approximation, used to derive Eq. (3), to be accurate are

$$\frac{\alpha\,Z}{\beta_1} \ll 1, \quad \frac{\alpha\,Z}{\beta_2} \ll 1 \quad (5)$$

involving both the initial and final electron velocities, β_1 and β_2, respectively. Equations (5) imply that Eq. (3) will fail (i) if the initial electron kinetic energy is too low and (ii) if the final electron kinetic energy is too low. Both (i) and (ii) must hold simultaneously. Here this is not a big concern because we consider electron kinetic energies above 1 MeV and use Eq. (3) only to determine the screening correction, which goes to zero close to the tip (i.e., $k \to \epsilon_1 - 1$ or $\epsilon_2 \to 1$).

C. The Furry-Sommerfeld-Maue wave functions

The Furry-Sommerfeld-Maue wave functions are not exact solutions of the Dirac equation in a pure Coulomb field, but only approximations. The basic idea is to transform the Dirac equation, a first-order PDE, into a second-order PDE, which has a dominant term plus other terms that are suppressed by $\alpha\,Z$ and $(\alpha\,Z)^2$. The dominant term of the second-order PDE has the same structure as the nonrelativistic Schrödinger PDE and can be solved in closed form arriving at a wave function ψ_0, which is taken as the expansion point:

$$\Psi = \psi_0 + (\alpha\,Z)\,\psi_1 + (\alpha\,Z)^2\,\psi_2 + \cdots. \quad (6)$$

The next correction term ψ_1 is added to Eq. (6) so that Ψ satisfies the second-order PDE (equivalent to the Dirac equation) including, beyond the dominant term, the next one of order $\alpha\,Z$. Furry [16] and, independently, Sommerfeld and Maue [17] were able to obtain a closed form for ψ_1 and found the solution

$$\Psi_{\rm FSM} = \psi_{\rm a} + \psi_{\rm b} \quad (7)$$

where $\psi_{\rm a} = \psi_0$ and $\psi_{\rm b} = (\alpha\,Z)\,\psi_1$. The expression found by Sommerfeld and Maue, although mathematically equivalent, was actually simpler. It is generally accepted that this feat cannot be repeated and a closed form cannot be found for ψ_2. When $\Psi_{\rm FSM}$ is substituted back into the full Dirac equation, the latter is satisfied up to terms of order

$$\frac{(\alpha\,Z)^2}{r}\,\sin\left(\frac{\theta}{2}\right) \quad (8)$$

where θ is the angle between $\boldsymbol{p}$ and $\boldsymbol{k}$. It is clear that the Furry-Sommerfeld-Maue wave functions are accurate for low-Z elements at all angles and all energies; while for high-Z elements they can be used only at small angles. The latter is generally not a severe problem at high energies because the cross section is dominated by small angles $\theta \approx 1/\epsilon$.

Bethe and Maximon [18,27] were the first to employ the Furry-Sommerfeld-Maue wave functions to calculate the bremsstrahlung TDCS with the matrix element

$$M_{\rm BM} = M_{\rm 2a,1a} + M_{\rm 2a,1b} + M_{\rm 2b,1a} \quad (9)$$

where the subscripts indicate whether $\psi_{\rm a}$ or $\psi_{\rm b}$ are used for the initial, subscript (1), or the final, subscript (2), states. It is important to note that, once the integrals are performed, all three contributions to the matrix element $M_{\rm BM}$ turn out to be of order $\alpha\,Z$: hence the use of $\psi_{\rm a} = \psi_0$ alone would lead to an inconsistent result. Contrarily to the Born approximation, here ψ_0 contributes to the matrix element, but, consistently with the Born approximation, the lowest-order contribution is of order $\alpha\,Z$. So, being the error on $\Psi_{\rm FSM}$ of order $(\alpha\,Z)^2$ when compared to the exact result, it does not make sense to include $M_{\rm 2b,1b}$ in $M_{\rm BM}$ because other contributions of the same order would be missing. The cross section corresponding to the matrix element of Eq. (9) is obviously of order $(\alpha\,Z)^2$.

Elwert and Haug [23] were the first to complete the calculation of the TDCS starting from Eq. (9) without any further approximation, arriving to the expression

$$\frac{d^3\sigma_{\rm LO}}{dk\,d\Omega_k\,d\Omega_{p_2}} = \frac{\alpha\,Z^2\,r_0^2}{\pi^2}\,\frac{k\,p_2}{p_1}\,N\Big([\epsilon_1\,\epsilon_2 - 1 - (\boldsymbol{p}_1\cdot\hat{\boldsymbol{k}})\,(\boldsymbol{p}_2\cdot\hat{\boldsymbol{k}})]\,|J_1|^2 + [\epsilon_1\,\epsilon_2 + 1 + (\boldsymbol{p}_1\cdot\hat{\boldsymbol{k}})\,(\boldsymbol{p}_2\cdot\hat{\boldsymbol{k}})]\,(|\boldsymbol{J}_2|^2 + |\boldsymbol{J}_3|^2) + 2\,{\rm Re}\{(\boldsymbol{J}_3 - \boldsymbol{J}_2)\cdot[\boldsymbol{p}_1\,(\boldsymbol{J}_2\cdot\hat{\boldsymbol{k}})\,(\boldsymbol{p}_2\cdot\hat{\boldsymbol{k}}) - \boldsymbol{p}_2\,(\boldsymbol{J}_3\cdot\hat{\boldsymbol{k}})\,(\boldsymbol{p}_1\cdot\hat{\boldsymbol{k}})] - (\epsilon_1\,\epsilon_2 + 1 + \boldsymbol{p}_1\cdot\boldsymbol{p}_2)\,(\boldsymbol{J}_2\cdot\hat{\boldsymbol{k}})\,(\boldsymbol{J}_3^\star\cdot\hat{\boldsymbol{k}})$$

$$+(\boldsymbol{J}_2\cdot\boldsymbol{p}_1)(\boldsymbol{J}_3^\star\cdot\boldsymbol{p}_2)-(\boldsymbol{J}_2\cdot\boldsymbol{p}_2)(\boldsymbol{J}_3^\star\cdot\boldsymbol{p}_1)+\epsilon_1\,J_1^\star\,[\boldsymbol{J}_3\cdot\boldsymbol{p}_2-(\boldsymbol{J}_2\cdot\hat{\boldsymbol{k}})(\boldsymbol{p}_2\cdot\hat{\boldsymbol{k}})]$$
$$+\epsilon_2\,J_1^\star\,[\boldsymbol{J}_2\cdot\boldsymbol{p}_1-(\boldsymbol{J}_3\cdot\hat{\boldsymbol{k}})(\boldsymbol{p}_1\cdot\hat{\boldsymbol{k}})]+(\boldsymbol{J}_2\cdot\boldsymbol{J}_3)\,[\boldsymbol{p}_1\cdot\boldsymbol{p}_2-(\boldsymbol{p}_1\cdot\hat{\boldsymbol{k}})(\boldsymbol{p}_2\cdot\hat{\boldsymbol{k}})]\}\Big) \tag{10}$$

where $\hat{\boldsymbol{k}}=\boldsymbol{k}/k$ and the other auxiliary quantities are defined next. The subscript LO in Eq. (10) indicates that this is the leading-order result for the TDCS obtained using the Furry-Sommerfeld-Maue wave functions without any other approximation, in particular without the high-energy (i.e., $\epsilon_1\gg1$, $\epsilon_2\gg1$, and $k\gg1$) and small-angle assumptions adopted by Bethe and Maximon [18].

Elwert and Haug [23] were able to investigate analytically several properties of Eq. (10); the most relevant, in the present context, is that, for low-Z atoms, the high-energy limit (i.e., $\epsilon_1\gg1$ and $\epsilon_2\gg1$) of Eq. (10) is the Bethe-Heitler formula without screening (i.e., $F=0$). Because Eq. (10) is, under such conditions, equivalent to the Bethe-Heitler formula, this justifies, at least for low-Z atoms and at high energies, the use of Eq. (1) to include the effect of screening in Eq. (10), as we will do here. The analytic properties demonstrated by Elwert and Haug were employed to implement a series of numerical tests (to be described elsewhere [6,28]) to ensure that no typographic errors are present in Eq. (10) and that our implementation is correct.

Higher-order corrections within the Born approximation were considered by several authors, but the calculations are difficult because of the presence of divergences and in the end they do not improve the agreement with data [24]. They will be discussed in more detail elsewhere [6]. Moreover, none of the available results include the effect of screening and are hence not particularly useful for the present scope: to calculate the DDCS at all photon energies and angles, screening must be taken into account. For this reason, here we prefer to use the formula by Roche, Ducos, and Proriol [24], who included higher-order corrections within the more accurate framework of the Furry-Sommerfeld-Maue wave functions, but necessarily neglected screening. Their result is still nowadays the best available for higher-order corrections within such an approach. Screening is then taken into account according to Eq. (1), as suggested by Haug [8]: this is not a fully consistent procedure because, in doing so, the higher-order corrections are considered for the interaction of the electron with the Coulomb field of the nucleus but not for the screening effect of the atomic electrons. A detailed comparison with data is hence needed to validate the present procedure.

Roche, Ducos, and Proriol [24] considered initial and final electron wave functions of the form

$$\Psi=\Psi_{\rm FSM}+\psi_{\rm c}=\psi_{\rm a}+\psi_{\rm b}+\psi_{\rm c} \tag{11}$$

where $\psi_{\rm c}=(\alpha\,Z)^2\,\psi_2$. As mentioned, no closed expression is known for ψ_2, but Roche, Ducos, and Proriol neglected all terms of order higher than $(\alpha\,Z)^2$ in the PDE for ψ_2 and found a solution [see Eq. (2.10) of Ref. [24]] valid at high energies (i.e., $\epsilon\gg1$). Because their result is from the beginning only valid for $\epsilon\gg1$, it does not make sense to invest any effort in including contributions to the matrix element that are not important under such a condition. Bethe and Maximon [18] have shown that (a) $M_{\rm 2b,1b}$ is of order $\epsilon^{-2}\ln\epsilon$; (b) $M_{\rm 2a,1c}$ and $M_{\rm 2c,1a}$ are of order ϵ^{-1}; and (c) all other contributions beyond those included in Eq. (9) and those mentioned in (a) and (b) above lead to terms of higher orders in $\alpha\,Z$. For this reason, Roche, Ducos, and Proriol [24] limited their calculations to

$$M_{\rm RDP}=M_{\rm BM}+M_{\rm c}, \tag{12a}$$
$$M_{\rm c}=M_{\rm 2a,1c}+M_{\rm 2c,1a}, \tag{12b}$$
$$|M_{\rm RDP}|^2=|M_{\rm BM}|^2+2\,{\rm Re}(M_{\rm BM}^\star\,M_{\rm c})+|M_{\rm c}|^2 \tag{12c}$$

where now $M_{\rm RDP}$ contains all terms up to order $(\alpha\,Z)^2$ relevant for $\epsilon\gg1$. Roche, Ducos, and Proriol evaluated the TDCS from Eq. (12c) without any further approximations; however, this is not a fully consistent procedure because now $M_{\rm RDP}$ contains contributions of different orders in $\alpha\,Z$ (contrary to $M_{\rm BM}$ that is restricted to those of order $\alpha\,Z$). In fact, while the second term in Eq. (12c) contains all the contributions of order $(\alpha\,Z)^3$ relevant at high energies, the third term in Eq. (12c) only contains some contributions of order $(\alpha\,Z)^4$. This is true for the TDCS, as well: the expression proposed by Roche, Ducos, and Proriol contains all contributions of order $(\alpha\,Z)^3$ relevant for $\epsilon\gg1$. However, to improve the agreement with measurements [24], these authors included also the evaluation of some contributions of order $(\alpha\,Z)^4$: those originated from $|M_{\rm c}|^2$ in Eq. (12c) and the full form of J_1, $\boldsymbol{J}_2$, and $\boldsymbol{J}_3$ [note that the expansion parameter $\alpha\,Z$ appears inside J_1, $\boldsymbol{J}_2$, and $\boldsymbol{J}_3$, see Eqs. (14d)–(14f), through a_1 and a_2, see Eqs. (14b) and (14c)] and proposed to evaluate the correction to the TDCS as

$$\frac{d^3\sigma_{\rm NLO}}{dk\,d\Omega_k\,d\Omega_{p_2}}=\alpha^2\,Z^3\,r_0^2\,\frac{k\,p_2\,(\boldsymbol{q}\cdot\boldsymbol{k})}{p_1\,q\,D_1\,D_2}\,N\left(\frac{2}{\pi}\,{\rm Re}(\{[\epsilon_1\,\epsilon_2-1-(\boldsymbol{p}_1\cdot\hat{\boldsymbol{k}})(\boldsymbol{p}_2\cdot\hat{\boldsymbol{k}})]\,J_1+\epsilon_1\,[\boldsymbol{J}_3\cdot\boldsymbol{p}_2-(\boldsymbol{J}_2\cdot\hat{\boldsymbol{k}})(\boldsymbol{p}_2\cdot\hat{\boldsymbol{k}})]+\epsilon_2\,[\boldsymbol{J}_2\cdot\boldsymbol{p}_1-(\boldsymbol{J}_3\cdot\hat{\boldsymbol{k}})(\boldsymbol{p}_1\cdot\hat{\boldsymbol{k}})]\}\,e^{i\Phi})+\alpha\,Z\,\frac{\boldsymbol{q}\cdot\boldsymbol{k}}{q\,D_1\,D_2}\,[\epsilon_1\,\epsilon_2-1-(\boldsymbol{p}_1\cdot\hat{\boldsymbol{k}})(\boldsymbol{p}_2\cdot\hat{\boldsymbol{k}})]\right). \tag{13}$$

The auxiliary quantities present in Eqs. (10) and (13) are given by

$$N=\frac{4\pi^2\,a_1\,a_2}{(e^{2\pi\,a_1}-1)\,(1-e^{-2\pi\,a_2})}, \tag{14a}$$
$$a_1=(\epsilon_1/p_1)\,\alpha\,Z, \tag{14b}$$
$$a_2=(\epsilon_2/p_2)\,\alpha\,Z, \tag{14c}$$
$$J_1=2\left(\frac{\epsilon_2}{D_1}-\frac{\epsilon_1}{D_2}\right)\frac{V+i\,a_2\,x\,W}{q^2}+2\,i\,\frac{(1-x)\,W}{D_1\,D_2}\times\left[\epsilon_1\,a_2\left(\frac{\mu}{D_2}-1\right)-\epsilon_2\,a_1\left(\frac{\mu}{D_1}+1\right)\right], \tag{14d}$$

$$\boldsymbol{J}_2 = \frac{V + i\,a_2\,x\,W}{D_2\,q^2}\,\boldsymbol{q} - \frac{i\,a_2\,(1-x)\,W}{D_1\,D_2}\left[\left(\frac{\mu}{D_2}-1\right)\boldsymbol{q} - \frac{\boldsymbol{P}}{p_1}\right], \tag{14e}$$

$$\boldsymbol{J}_3 = \frac{V + i\,a_2\,x\,W}{D_2\,q^2}\,\boldsymbol{q} - \frac{i\,a_1\,(1-x)\,W}{D_1\,D_2}\left[\left(\frac{\mu}{D_1}+1\right)\boldsymbol{q} - \frac{\boldsymbol{P}}{p_2}\right], \tag{14f}$$

$$V = F(-i\,a_1, i\,a_2; 1; x), \tag{14g}$$

$$W = F(1 - i\,a_1, 1 + i\,a_2; 2; x), \tag{14h}$$

$$x = 1 - \frac{D_1\,D_2}{\mu\,q^2}, \tag{14i}$$

$$D_1 = 2\,k\,(\epsilon_1 - p_1\,\cos\theta_1), \tag{14j}$$

$$D_2 = 2\,k\,(\epsilon_2 - p_2\,\cos\theta_2), \tag{14k}$$

$$\mu = 2\,(\epsilon_1\,\epsilon_2 + p_1\,p_2 - 1), \tag{14l}$$

$$\boldsymbol{P} = p_1\,\boldsymbol{p}_2 + p_2\,\boldsymbol{p}_1, \tag{14m}$$

$$\Phi = a_1\,\ln\left(\frac{q^2}{D_2}\right) - a_2\,\ln\left(\frac{\mu}{D_2}\right) \tag{14n}$$

where $F(a,b;c;z)$ is the hypergeometric function of complex arguments [29,30].

Although, Eq. (13) has the subscript NLO, the discussion about its mixed order should be kept in mind. Moreover, the expression of ψ_c and the selection of the matrix elements included is meaningful only at high energies both for the initial and final electrons: Eq. (13) cannot be expected to be accurate close to the tip. It is also important to note that, while Eq. (10) and the sum of Eqs. (10) and (13) represent TDCSs and must be positive, Eq. (13) is a correction term and, as such, it is not a cross section and does not have to be positive.

D. Summary of the approximations involved

To summarize, in the present work, following Eq. (1), we will calculate the DDCS for bremsstrahlung by correcting the sum of Eqs. (10) and (13) with the difference between Eq. (3) with and without screening, all integrated over the final electron solid angle. This includes the following approximations.

(i) The interaction with the Coulomb field of the nucleus has been described with the Furry-Sommerfeld-Maue wave functions, which are accurate for low-Z elements at all energies and angles. For high-Z elements, they are a good approximation only at sufficiently small angles. Within these limitations, the formula by Elwert and Haug for the TDCS, Eq. (10), is exact.

(ii) The higher-order corrections to the interaction with the Coulomb field of the nucleus have been included with the result obtained by Roche, Ducos, and Proriol [24], Eq. (13). This should improve the limitations mentioned in the previous item for high-Z elements, but their expression is valid only when the initial and final electrons are ultrarelativistic. Moreover, their calculation is consistent up to order $(\alpha\,Z)^3$, but they include some terms of order $(\alpha\,Z)^4$.

(iii) The screening by the atomic electrons has been included with the Olsen-Maximon-Wergeland additivity rule, Eq. (1), which has been proven only for high energies within the WKB approximation.

(iv) The expression obtained within the first Born approximation by Maximon, de Miniac, Aniel, and Ganz [25], Eq. (3), has been used for calculating the screening correction. Thus, higher orders are not included for the screening by the atomic electrons.

III. NUMERICAL IMPLEMENTATION

Equations (3), (10), and (13) have been implemented into a dedicated FORTRAN program. The heaviest computational cost is the evaluation of the hypergeometric function: since the first two arguments are complex, we could not use a simpler routine and had to resort to a more general one published by Press, Flannery, Teukolsky, and Vetterling [31]. To prevent the calculation time from growing prohibitively when the argument x in Eqs. (14g) and (14h) is close to 1, a transformation was used relating $F(a,b;c;z)$ to $F(a,b;a+b-c+1;1-z)$, $F(c-a,c-b;c-a-b+1;1-z)$, and seven evaluations of the Gamma function of complex argument, as suggested by Roche, Ducos, and Proriol [24] [see Eq. (9.131.2) in Ref. [30]].

To obtain a DDCS or a SDCS, a numerical integration is performed with the multidimensional adaptive Gaussian quadrature routine DADMUL [32] included in the CERN Program Library. For all the results presented here, the requested relative accuracy is $\varepsilon_{\rm rel} = 10^{-5}$.

An extensive set of tests has been performed to check the correctness of the implementation of the analytic formulae as well as the accuracy of the error estimate employed by the adaptive Gaussian quadrature routine. A comparison of the SDCSs obtained from Eq. (10) with benchmark values published by Bernhardi *et al.* [33] has also been done. They will be described in detail elsewhere [6,28].

IV. SOME GENERAL FEATURES OF THE CALCULATIONS

Before attempting a comparison with the experimental data, it is useful, for streamlining the discussion, to illustrate a few general features of the calculations. To give an intuitive picture, the semiclassical Weizsäcker-Williams approach can be adopted (see, e.g., the textbook by Jackson [34]). In this description, the electron emits the photon at a characteristic impact parameter b given by $b \approx \lambda\!\!\!^{-}_C/q$ where $\lambda\!\!\!^{-}_C$ is the reduced Compton wavelength of the electron. Equivalently, one can say that the matrix element given by Fermi's "golden rule" contains an integral over the whole space the argument of which oscillates strongly away from the region where $b \approx \lambda\!\!\!^{-}_C/q$, that ends up giving most of the contribution. Combining this with the considerations given at the beginning of Sec. II, it is possible to understand that the interaction with the nuclear Coulomb field has to be described accurately close to the nucleus (i.e., $q \gg 1$) while the effect of screening by the atomic electrons is important far from the nucleus (i.e., $q \ll 1$). Consequently, higher-order corrections are also expected to be more important for high-Z elements and for $q \gg 1$.

An explicit link with the characteristics to be observed in the comparisons with data requires one to express the conditions on q in a different way: for low radiated photon energies and small emission angles typically $q \ll 1$, while close to the tip and at large emission angles $q \gg 1$. Intermediate situations are less clean cut. Let us analyze the case where $\epsilon_1 \approx 3.33$, the lowest energy considered here, and $\theta_k = 0$: the momentum transfer q increases with k and reaches the maximum value of $q \approx 0.883$ at $k = \epsilon_1 - 1$ (i.e., the tip of the spectrum). This means that $b \approx 1.13\,\lambda\!\!\!^{-}_{C}$, that is relatively close to the nucleus ($\approx 1.13\,\alpha$ times the Bohr radius) resulting in a negligible screening correction at the tip. The same conclusion is valid for all the other cases that will be analyzed in Sec. V, because ϵ_1 is higher or θ_k larger.

Concerning the DDCS, one more feature is important: the first Born approximation, like for example Eq. (3), always gives a zero value at the tip: only the use of Eqs. (10) and (13), derived with the Furry-Sommerfeld-Maue wave functions, leads to a finite result. This is also the region of the spectrum where a direct test of the improvement brought by the use of the Furry-Sommerfeld-Maue wave functions is the most direct because of the absence of screening, according to the discussion in the previous paragraph. The expression for the higher-order corrections found by Roche, Ducos, and Proriol [24] is, unfortunately, not valid close to the tip (see Sec. II).

Finally, one more general comment of interest for the following discussion can be made about Eq. (1). The second term on the right-hand side is, as mentioned, the correction due to the screening by the atomic electrons evaluated with the first Born approximation. The difference of the exact cross section for a pure Coulomb field, the first term on the right-hand side, from the cross section given by the first Born approximation without screening [i.e., the integral of Eq. (3) with $F = 0$ over the final electron solid angle] is commonly referred to in the literature as the Coulomb correction.

V. COMPARISON WITH DATA FOR DDCSS AT A FEW MeV

The angular distribution of the bremsstrahlung photons emitted by few-MeV electrons is rather broad so that DDCSs can be measured. There are three datasets available in the literature for electrons with kinetic energies of 1 MeV or above and thin targets: those by Motz [35], Starfelt and Koch [36], and Rester and Dance [37]. There are other papers where thick targets were employed, but they cannot be used to compare directly with theory. The mentioned authors did a rather thorough work, even by current standards, where they applied (i) a correction for the pulse pileup, (ii) a correction for the background, (iii) a correction for the detector response function, and (iv) a correction for the detector efficiency and acceptance. A more detailed discussion of the procedures employed can be found in the original papers.

As a matter of fact, there are measurements by Motz [35] and by Rester and Dance [37] that can be compared directly and, unfortunately, in some cases, do not agree. This somewhat weakens the strength of the experimental results, but there is no way to improve the situation at the moment of writing. The data by Rester and Dance are in better overall agreement with theory and for this reason we will not examine those by Motz here (a comparison will be shown elsewhere [6]). Moreover, both Starfelt and Koch [36] and Rester and Dance [37] covered several target-electron energy-photon emission angle combinations, but to save space only a few representative cases are shown here in Figs. 1 and 2: we have selected one low-Z element (Al), one intermediate-Z element (Sn is present only in the data by Rester and Dance), and one high-Z element (Au). Starfelt and Koch considered also Be, but in this case the contribution of electron-electron bremsstrahlung is too high for the present calculations (including only nuclear bremsstrahlung) to be accurate. We have also chosen two representative angles: one small (shown on the left panels) and one large (shown on the right panels). A full comparison with the complete datasets will be included in a review to be published shortly elsewhere [6]. As a last warning, we stress that the experimental values presented here have been read by us from the original figures (that employ logarithmic scales) by a special program. The statistical and systematic errors, represented, respectively, with error bars and a contour in the figures, have been calculated, respectively, as the quadratic and linear sums of the individual contributions listed in the original publications.

The more familiar physical units have been used in the figures, introducing the initial electron kinetic energy $T_{e1} = m_e c^2\,(\epsilon_1 - 1)$ and the radiated photon energy $E_{ph} = m_e c^2\,k$ and angle $\theta_{ph} = \theta_k\,180^\circ/\pi$.

The main conclusions that can be drawn from Figs. 1 and 2 (and are fully consistent with the other cases not shown here) are the following.

(i) The agreement for low-Z elements (Al) is good over all energies, T_{e1}, and all angles, θ_{ph}, for the complete spectrum: the calculations pass within the statistical error bars in most cases and within the systematic error contours in all others (see Figs. 1 and 2).

(ii) The situation is rather different for high-Z elements. The accuracy of the description of the interaction with the Coulomb field of the nucleus can be directly evaluated by looking at the region of the spectrum close to the tip, where the screening correction does not affect the calculations because it is absent (see Sec. IV). The reader should also remember that the first Born approximation gives always a zero DDCS at the tip (see Sec. IV): the finite values visible in the figures are a result of the use of the Furry-Sommerfeld-Maue wave functions. While for Cu (not shown) and Sn the agreement is still within the uncertainties, for Au the predicted values are at the lower border of the claimed uncertainty margin, if not below [see Fig. 1: the effect discussed here is actually mixed with the tendency to underestimate the DDCS at large angles to be discussed in item (iii)]. The data by Starfelt and Koch extend beyond the beam kinetic energy because of detector resolution (see Fig. 2), indicating that their deconvolution of the response function was not accurate enough in this region. So it is not clear how reliable are their values for the DDCS close to the tip.

(iii) The most striking aspect of the calculations is a significant underestimation of the data for high-Z elements (Au) at large angles, well beyond the experimental uncertainties (see Figs. 1 and 2). The beginning of this tendency already

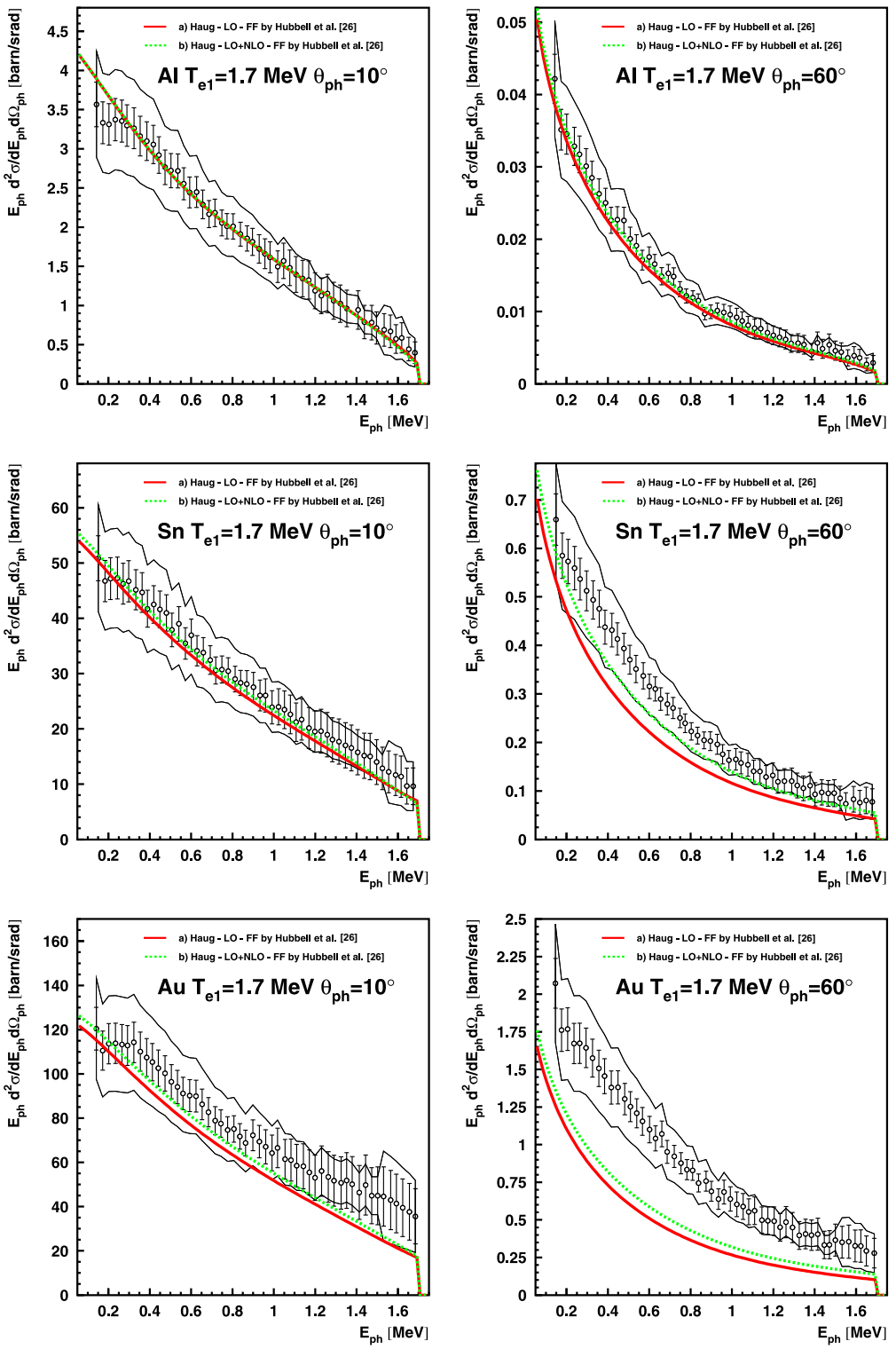

FIG. 1. Comparison of the analytic formulae including the effect of the screening and the Coulomb correction at the LO and NLO with the data by Rester and Dance [37] (open circles). The error bars and the contour represent the quadratic and linear sums of the statistical and systematic errors quoted in Ref. [37], respectively.

appears for Cu (not shown) and Sn (see Fig. 1) in the data by Rester and Dance. A small effect is present also for Al in the same set of data (see again Fig. 1). Because such a feature is present along the complete spectrum, it is harder to disentangle the contribution of the screening and Coulomb corrections. However, the fully consistent behavior up to the tip offers a hint that the main origin is a limitation of the latter [see item (ii)]. Although other explanations are possible, as we will show in our review [6], none is quantitatively consistent. In particular, we have performed accurate calculations of

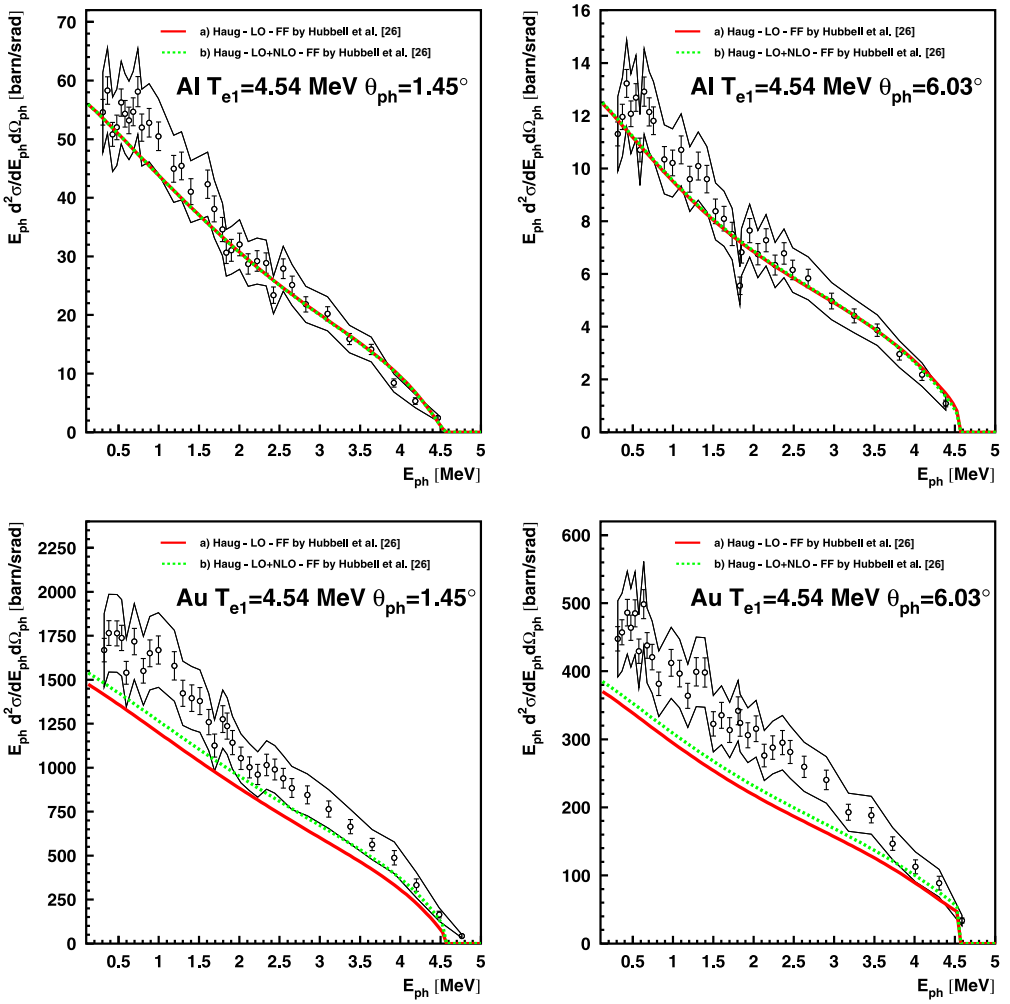

FIG. 2. Comparison of the analytic formulae including the effect of the screening and the Coulomb correction at the LO and NLO with the data by Starfelt and Koch [36] (open circles). The error bars and the contour represent the quadratic and linear sums of the statistical and systematic errors quoted in Ref. [36], respectively.

multiple scattering for the actual target thicknesses employed in the measurements and evaluated the convolution with the bremsstrahlung DDCS of Figs. 1 and 2 to take into account that the emission and observation angles of the photons can be different: we did not find any appreciable distortion for Figs. 1 and 2. As a matter of fact, the effect of multiple scattering is largest when $\theta_{\rm ph}$ is very close to zero and for this reason we did not select $\theta_{\rm ph} = 0^\circ$ as the smallest angle in Figs. 1 and 2. So the most plausible conclusion is indeed that the underestimation is due to the approximations resulting from the use of the Furry-Sommerfeld-Maue wave functions. Although Eq. (8) indicates that these wave functions are less accurate for high-Z elements and large angles, the link with the DDCS is not immediate because it involves an integral over the final electron solid angle.

(iv) A tendency of the calculations to underestimate the data by Starfelt and Koch at low photon energies, $E_{\rm ph}$, is visible in Fig. 2 for both Al and Au. As a matter of fact, this is the region of the spectrum that is most sensitive to the screening correction (see Sec. IV), that could then be too large. However, it is important to notice that because there are no radioactive sources that produce γ rays with energies close to 4.54 MeV Starfelt and Koch had to rely on Monte Carlo simulations to determine the detector response function to be deconvoluted from the measurements [36]. This renders their results more uncertain and a new experiment would be necessary to clarify this issue.

(v) Some general tendencies of the NLO correction can be observed in Figs. 1 and 2: (a) the NLO correction is small for low-Z elements (Al), as expected; (b) for fixed $T_{\rm e1}$, $\theta_{\rm ph}$, and $E_{\rm ph}$, the NLO correction increases with Z, as expected; (c) for fixed Z, $T_{\rm e1}$, and $E_{\rm ph}$, the NLO correction increases with angle: this is less intuitive but can be understood in the framework of the mentioned Weizsäcker-Williams approach, because increasing momentum transfers correspond to photons emitted closer to the nucleus (see Sec. IV); and (d) finally, for fixed Z, $T_{\rm e1}$, and $\theta_{\rm ph}$, the NLO correction is approximately constant with $E_{\rm ph}$, eventually displaying a tendency to decrease close to the tip [where Eq. (13) at any rate cannot be expected to be accurate]. This constancy is a general feature that remains true even at higher energies and for SDCSs: it will be discussed in more detail in Sec. VI.

Concerning the comparison with the data by Rester and Dance, for low-Z and intermediate-Z elements (Al, see Fig. 1; Cu, not shown; and Sn, see Fig. 1), the NLO correction improves the agreement at large angles. Its magnitude increases from Al to Sn and becomes approximately comparable to the experimental uncertainties for Sn: new measurements with improved accuracy would help to establish the correctness of the calculations. In the data by Starfelt and Koch for low Z (Al), no effect of the NLO correction is visible, possibly because the angle is not large enough (see Fig. 2). For high-Z elements (Au, see Figs. 1 and 2), the NLO correction goes in the right direction reducing the underestimation at large angles, but its magnitude is too small to significantly improve the situation and the disagreement remains even when considering the experimental uncertainties. At least for the data by Rester and Dance, the inaccuracy of Eq. (13) for electrons that are not relativistic can be a problem.

VI. COMPARISON WITH DATA FOR SDCSS AT HUNDREDS OF MeV

For electrons with kinetic energies above approximately 10 MeV, the angular distribution of the bremsstrahlung photons is narrowly focused forward and DDCSs cannot be easily measured. The preferred experimental procedure is rather to deflect the electron beam after the target and intercept all the emitted photons with a detector or to measure the energy spectrum of the electrons after irradiation, so that SDCSs are obtained. This has the consequence that even with thin targets the emission of multiple photons has to be taken into account to reproduce the data [38]. Moreover, because the energies are well above threshold, photon absorption by pair production in the target has also to be included [38].

One of the most striking features of nuclear bremsstrahlung is that a more accurate treatment of the interaction with the Coulomb field of the nucleus does not converge, for intermediate- and high-Z elements, to the first Born approximation result even in the high-energy limit, as first discovered by Bethe and Maximon [18] employing the Furry-Sommerfeld-Maue wave functions. This is not particularly intuitive especially when considering the presence of screening. Figure 3 shows the Coulomb correction defined as the difference of the nuclear bremsstrahlung SDCS, $(d\sigma/dk)^{\rm screened}_{\rm exact}$, obtained by integrating numerically the TDCS given by Eq. (10) or by Eqs. (10) and (13), with screening included via Eq. (1), from the first Born approximation result with screening, $(d\sigma/dk)^{\rm screened}_{\rm Born}$, obtained by integrating numerically the TDCS given by Eq. (3). The case considered is that of 100-MeV electrons impinging on Au. The AFF employed is the one by Hubbell and collaborators [26]. A special representation has been adopted, as first proposed by Seltzer and Berger [39], where this difference is normalized to $(d\sigma/dk)^{\rm screened}_{\rm exact}$ itself,

$$C_{\rm C} = \frac{\left(\frac{d\sigma}{dk}\right)^{\rm screened}_{\rm exact} - \left(\frac{d\sigma}{dk}\right)^{\rm screened}_{\rm Born}}{\left(\frac{d\sigma}{dk}\right)^{\rm screened}_{\rm exact}} , \qquad (15)$$

and plotted as a function of the final electron kinetic energy $T_{\rm e2} = m_{\rm e}c^2\,(\epsilon_2 - 1)$. The main advantage of these variables is that the curves shown in Fig. 3 do not depend on $T_{\rm e1}$, when above ≈100 MeV [39]. Moreover, the extension of Fig. 3 towards higher values of $T_{\rm e2}$ is again particularly simple, because the ratios, so expressed, remain constant [39]: i.e., at low $E_{\rm ph}$, the Coulomb correction does not change the shape of the radiated photon spectrum given by the first Born approximation with screening, but only leads to a reduction by a fraction that depends only on Z (for Au it is ≈9%, see Fig. 3). For this reason, at high $T_{\rm e1}$, it is an approximation valid over most of the spectrum to reabsorb the Coulomb correction into a redefinition of the radiation length. Seltzer and Berger limited their work to the LO [39]; here we show that the inclusion of the NLO brings the calculated SDCS back close to the first Born approximation result: the final reduction for Au is diminished from ≈9% to ≈2%. In terms of radiation length, this means that the NLO is closer to the Bethe-Heitler value than the LO. It is important to remember that Eq. (13) is not expected to be valid when $T_{\rm e2}$ approaches zero (see Sec. II) so that neither is the dashed curve shown in Fig. 3.

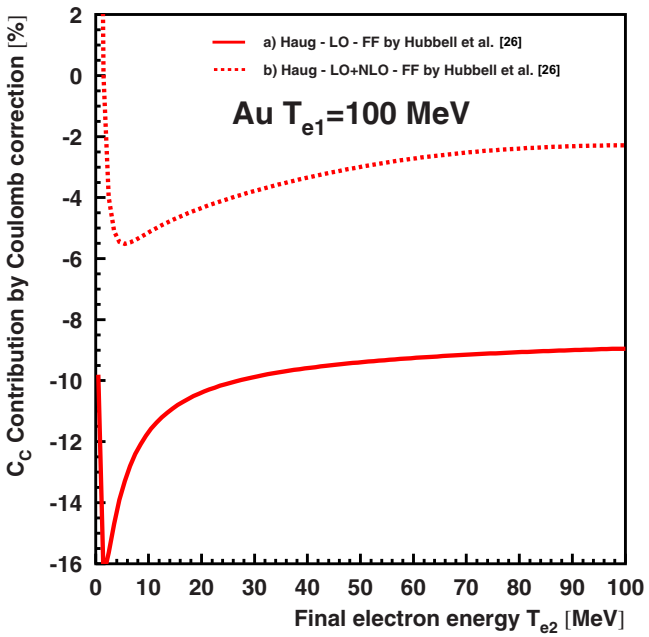

FIG. 3. Contribution of the Coulomb correction to the nuclear bremsstrahlung SDCS including the effect of the screening; see Eq. (15).

We scanned the literature for measurements of bremsstrahlung by electrons with energies above ≈100 MeV, where the Coulomb correction is constant, and below ≈1 GeV, where the Landau-Pomeranchuk-Migdal [40–42] effect can be neglected. We found four, all from the 1950s: one by Powell *et al.* [43], one by DeWire and Beach [44], one by Fisher [45], and one by Brown [46]. The works by Powell *et al.* [43] and by DeWire and Beach [44] only give the spectral shape in arbitrary units (for one element) and can hence not be used to test the Coulomb correction at high energies accurately, because, as shown in Fig. 3, over most of the spectrum a rescaling of the Bethe-Heitler result by a constant is a good approximation. The data by Fisher [45] suffer from some other limitations: (i) the beam energy was not well defined (see Fig. 2 of Ref. [45]) and (ii) the energy of the radiated photons was

deduced by measuring in a magnetic field the curvature of the tracks of the electrons leaving the target (and assuming that the missing primary energy is released in a single emission act). Because (i) would require us to convolute the calculations with the beam energy distribution (as indeed was done in Ref. [45] with simpler formulae; in the present case it would be quite laborious numerically) and because (ii) involves some corrections, with large uncertainties (mostly connected to the effect of the projection on the plane of the photographic image, see Ref. [45]), we prefer to disregard this publication. The work by Brown [46] was quite meticulous: the primary beam from a linear accelerator with a well-defined energy of $T_{e1} = 500$ MeV was used, the electrons after irradiation were deflected with a magnet, and the emitted photons were detected by pion photoproduction on a liquid hydrogen target. By defining very well the momentum of the accepted pions with an analyzing magnet, it was possible to select only photons with an energy of $E_{ph} = 234 \pm 6$ MeV. This value is comfortably located close to the middle of the photon spectrum, where the NLO correction given by Eq. (13) is valid. Brown did a relative measurement of the yields from Ta and U, adopting Cu as a reference, thus reducing the impact of experimental uncertainties (including those on the pion acceptance and photoproduction cross section). Moreover, because Brown selected in all cases a target with a thickness in units of a radiation length of 3%, the normalization to Cu minimized the effect of the emission of multiple photons and the attenuation by pair production (for exactly Bethe-Heitler bremsstrahlung and pair production cross sections, the spectra from a target with a constant thickness in units of radiation length would be the same for all elements, irrespective of multiphoton irradiation and of the attenuation by pair production [38]). To show clearly the magnitude of the Coulomb correction, Brown normalized the experimental SDCS $(d\sigma/dk)^{\rm exp}$ to the Bethe-Heitler formula with screening $(d\sigma/dk)^{\rm screened}_{\rm Born}$ and expressed his results with the ratio

$$R_{\rm C} = \left(\frac{\left(\frac{d\sigma}{dk}\right)^{\rm exp}}{\left(\frac{d\sigma}{dk}\right)^{\rm screened}_{\rm Born}}\right) \Big/ \left(\frac{\left(\frac{d\sigma}{dk}\right)^{\rm exp}}{\left(\frac{d\sigma}{dk}\right)^{\rm screened}_{\rm Born}}\right)_{\rm Cu} . \qquad (16)$$

This variable has the disadvantage of mixing measured and calculated quantities, which, in particular, depend on the choice of an AFF. Although Brown does not supply any further information, the sensitivity of the theoretical values to such details is relatively modest [6]. The same quantity $R_{\rm C}$ has also been calculated by replacing the measured SDCS with the best theoretical estimates proposed in the present work at the LO and NLO and is compared in Fig. 4 with the published data by Brown. The AFFs adopted in the calculations are again those by Hubbell and collaborators. The uncertainties quoted by Brown are not discussed in detail and in particular are not separated into statistical and systematic contributions: for this reason they are represented with a single error bar in Fig. 4.

Figure 4, like Fig. 3, shows that the NLO reduces the Coulomb correction at the LO and brings the SDCS closer to the Bethe-Heitler value. Surprisingly, the data by Brown agree better with the LO than with the NLO. This is apparently at odds with Fig. 1, where, to get agreement with data for high Z and large angles, the NLO should increase even more the DDCS (as a matter of fact beyond the Bethe-Heitler value); the

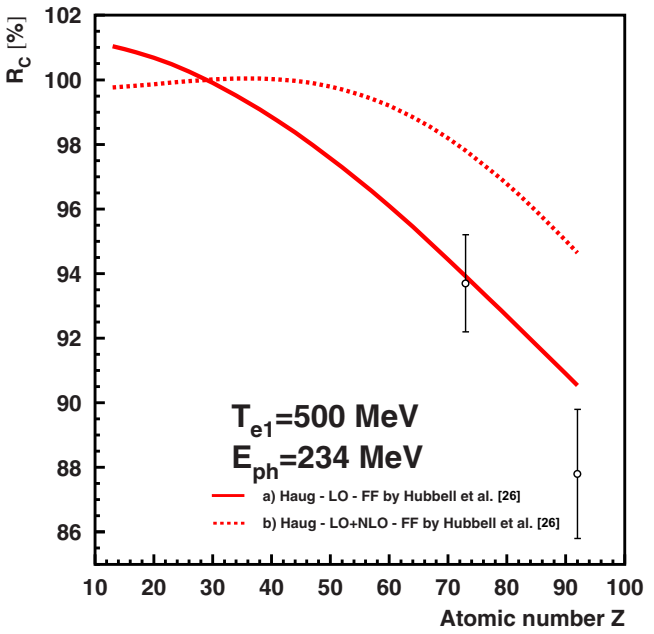

FIG. 4. Ratio of the nuclear bremsstrahlung SDCS to the first Born approximation result including the screening correction normalized to Cu; see Eq. (16). The experimental data with their error bars are those by Brown [46].

possible inconsistency between the experimental data warns against drawing definitive conclusions without collecting new measurements with modern equipment and with a rigorous quantification of the budget of uncertainties. This is even more true for the SDCSs at high energies by Brown, where discriminating the NLO from the LO is a matter of a few percent (once more we recall that the shape of the photon spectrum is not a useful observable in this context). It is also quite unexpected, on general grounds, that, e.g., for U, where $\alpha Z \approx 0.67$, the data leave essentially no room for the NLO. If the present experimental situation stands, there are only two possible aspects where the calculations of the NLO can be wrong.

(i) The Olsen-Maximon-Wergeland additivity rule [see the approximation (iii) in Sec. II D] may not work for higher-order corrections.

(ii) Higher orders have to be included also for screening and partially compensate those introduced for describing more accurately the interaction with the Coulomb field of the nucleus [see the approximation (iv) in Sec. II D].

It is important to remark that, on one hand, both issues listed above are very difficult to be tackled analytically, while, on the other hand, the number of partial waves needed at these energies cannot be dealt with numerically, as mentioned in the Introduction. Thus, it appears that reliable cross sections for nuclear bremsstrahlung cannot be obtained in the near future for electrons with energies above a few MeV impinging on high-Z elements.

VII. CONCLUSIONS AND OUTLOOK

The present paper has compared in detail a state-of-the-art analytic calculation for nuclear bremsstrahlung with the scarce

and old published data for DDCSs at a few MeV and SDCSs at higher energies. The interaction with the Coulomb field of the nucleus has been described with the Furry-Sommerfeld-Maue wave functions and the screening effect of the electronic cloud of the atom has been included with the Olsen-Maximon-Wergeland additivity rule. The distinctive feature of this work is a thorough analysis of higher-order corrections to the interaction with the Coulomb field of the nucleus employing the expression by Roche, Ducos, and Proriol. We stress once more that the energy range covered in the present paper has only been met at the lower end by modern numerical calculations employing partial wave expansions, so that no reference theoretical cross sections are available. The main conclusions are as follows:

(i) For few-MeV electrons and low-Z elements (Al), the agreement with data is rather good (the calculations match all the measurements within the quoted statistical and systematic uncertainties) for all photon emission angles and energies. This is not at all immediate: the correct finite value of the cross section at the tip cannot be obtained within the first Born approximation and the Furry-Sommerfeld-Maue wave functions are necessary, in particular the Elwert-Haug expression, which has been obtained without the ultrarelativistic and small-angle approximations. The higher-order corrections are small, but have a positive effect at large angles.

(ii) For few-MeV electrons and intermediate- to high-Z elements (Cu, Sn, and Au), a specific failure is present in the form of an underestimation of the DDCSs at large photon emission angles. It is most probably a consequence of the limitations resulting from the use of the Furry-Sommerfeld-Maue wave functions. The current procedure to treat higher-order corrections improves the situation for intermediate-Z elements, but still falls well below data for high-Z targets.

(iii) For impinging electron energies of hundreds of MeV and intermediate- to high-Z elements, the measured SDCSs agree with calculations only when higher orders are not included within the present approach. In fact, higher orders increase the predicted values well above the estimated uncertainty of the measurements. This situation appears to be in contradiction with the mentioned underestimation of the DDCS data for few-MeV electrons radiating photons at large angles. If this situation is confirmed by more accurate experiments, it would require a new way to include higher-order corrections. In particular, the Olsen-Maximon-Wergeland additivity rule may not be valid for higher orders, or a compensation could be present between higher-order corrections to the interaction with the Coulomb field of the nucleus and the screening effect of the atomic electrons.

ACKNOWLEDGMENTS

The authors are grateful to Prof. Leonard C. Maximon for many enriching discussions and suggestions. They are in debt to Prof. Nora Lia Maidana and Prof. Vito R. Vanin of the Instituto de Física da Universidade de São Paulo, Prof. José María Fernandez Varea of the Universitat de Barcelona, and Prof. Pietro Sona of the Università di Firenze for several enlightening comments. A.M. acknowledges support by Fundação de Amparo à Pesquisa do Estado de São Paulo (FAPESP) under Contract No. 2013/15634-5 as visiting professor at the Instituto de Física da Universidade de São Paulo.

[1] A. Sommerfeld, Ann. Physik **11**, 257 (1931).
[2] F. Sauter, Ann. Physik **20**, 404 (1934).
[3] H. A. Bethe and W. Heitler, Proc. R. Soc. A **146**, 83 (1934).
[4] H. A. Bethe, Proc. Cambridge Phil. Soc. **30**, 524 (1934).
[5] G. Racah, Nuovo Cimento **11**, 461 (1934).
[6] A. Mangiarotti and M. N. Martins (unpublished).
[7] K. Mork and H. Olsen, Phys. Rev. **140**, B1661 (1965).
[8] E. Haug, Rad. Phys. Chem. **77**, 207 (2008).
[9] H. K. Tseng and R. H. Pratt, Phys. Rev. A **3**, 100 (1971).
[10] R. H. Pratt, H. K. Tseng, C. M. Lee, and L. Kissel, Atom. Data Nucl. Data Tab. **20**, 175 (1977); **26**, 477(E) (1981).
[11] H. K. Tseng and R. H. Pratt, Phys. Rev. A **19**, 1525 (1979).
[12] V. A. Yerokhin and A. Surzhykov, Phys. Rev. A **82**, 062702 (2010).
[13] O. Kovtun, V. Tioukine, A. Surzhykov, V. A. Yerokhin, B. Cederwall, and S. Tashenov, Phys. Rev. A **92**, 062707 (2015).
[14] D. H. Jakubassa-Amundsen, Phys. Rev. A **82**, 042714 (2010).
[15] D. H. Jakubassa-Amundsen, Eur. Phys. J. D **62**, 177 (2011).
[16] W. H. Furry, Phys. Rev. **46**, 391 (1934).
[17] A. Sommerfeld and A. W. Maue, Ann. Physik (Leipzig) **22**, 629 (1935).
[18] H. A. Bethe and L. C. Maximon, Phys. Rev. **93**, 768 (1954).
[19] H. Olsen, L. C. Maximon, and H. Wergeland, Phys. Rev. **106**, 27 (1957).
[20] H. Olsen, Phys. Rev. **99**, 1335 (1955).
[21] H. Olsen and L. C. Maximon, Phys. Rev. **114**, 887 (1959).
[22] R. N. Lee, A. I. Milstein, V. M. Strakhovenko, and O. Ya. Schwartz, J. Exp. Theor. Phys. **100**, 1 (2005).
[23] G. Elwert and E. Haug, Phys. Rev. **183**, 90 (1969).
[24] G. Roche, C. Ducos, and J. Proriol, Phys. Rev. A **5**, 2403 (1972).
[25] L. C. Maximon, A. de Miniac, T. Aniel, and E. Ganz, Phys. Rep. **147**, 189 (1987).
[26] J. H. Hubbell, W. J. Veigele, E. A. Briggs, R. T. Brown, D. T. Cromer, and R. J. Howerton, J. Phys. Chem. Ref. Data **4**, 471 (1975); **6**, 615(E) (1977).
[27] A. Nordsieck, Phys. Rev. **93**, 785 (1954).
[28] A. Mangiarotti *et al.* (unpublished).
[29] M. Abramowitz and I. A. Stegun, *Handbook of Mathematical Functions with Formulas, Graphs and Mathematical Tables*, 9th ed. (Dover, New York, 1972).
[30] I. S. Gradshteyn and I. M. Ryzhik, *Tables of Integrals, Series and Products*, 6th ed. (Academic, New York, 2000).
[31] W. H. Press, B. P. Flannery, S. A. Teukolsky, and W. T. Vetterling, *Numerical Recipes in FORTRAN 77, The Art of Scientific Computing*, 2nd ed. (Cambridge University, Cambridge, England, 1992).
[32] A. C. Genz and A. A. Malik, J. Comput. Appl. Math. **6**, 295 (1980).
[33] K. Bernhardi, E. Haug, and K. Wiesemann, Atom. Data Nucl. Data Tab. **28**, 461 (1983).

[34] J. D. Jackson, *Classical Electrodynamics*, 3rd ed. (Wiley, New York, 1999).
[35] J. W. Motz, Phys. Rev. **100**, 1560 (1955).
[36] N. Starfelt and H. W. Koch, Phys. Rev. **102**, 1598 (1956).
[37] D. H. Rester and W. E. Dance, Phys. Rev. **161**, 85 (1967).
[38] A. Mangiarotti, P. Sona, S. Ballestrero, U. I. Uggerhøj, and K. Andersen, Nucl. Instr. Meth. Phys. Res. Sec. B **289**, 5 (2012).
[39] S. M. Seltzer and M. J. Berger, Nucl. Instr. Meth. Phys. Res. Sec. B **12**, 95 (1985).
[40] L. D. Landau and I. J. Pomeranchuk, Dokl. Akad. Nauk SSSR **92**, 535 (1953); available in English in L. D. Landau, *The Collected Papers of L. D. Landau*, edited by D. Ter Haar (Pergamon, New York, 1965), p. 586.
[41] L. D. Landau and I. J. Pomeranchuk, Dokl. Akad. Nauk SSSR **92**, 735 (1953); available in English in L. D. Landau, *The Collected Papers of L. D. Landau*, edited by D. Ter Haar (Pergamon, New York, 1965), p. 589.
[42] A. B. Migdal, Phys. Rev. **103**, 1811 (1956).
[43] W. M. Powell, W. Hartsough, and M. Hill, Phys. Rev. **81**, 213 (1951).
[44] J. W. DeWire and L. A. Beach, Phys. Rev. **83**, 476 (1951).
[45] P. C. Fisher, Phys. Rev. **92**, 420 (1953).
[46] K. L. Brown, Phys. Rev. **103**, 243 (1956).